Research on seismic absorption of high-speed railway segmental assembled round-end hollow pier with low yield point steel connection buckle

Hao Li[1], Yuanqing Xu[2], Hongjie Zhang[3], Shiyun Qi[4]
[1, 4]School of Civil Engineering, Beijing Jiaotong University, Beijing, China
[1, 3]Beijing Urban Construction Design and Development Group Co., Ltd, Beijing, China
[2]College of Civil Engineering, Hunan University, Hunan, China
[2]CCCC Highway Bridge National Engineering Research Centre Co., Ltd., Beijing, China
[1]Corresponding author
E-mail: [1]*19121063@bjtu.edu.cn*, [2]*xuyuanqing@bnerc.com*, [3]*yfzhj904@sina.com*, [4]*qsy101200@163.com*

Received 9 August 2022; received in revised form 8 December 2022; accepted 23 December 2022
DOI https://doi.org/10.21595/jve.2022.22859

Abstract. The research aims to enhance the seismic safety of the segmental assembled round end hollow pier (SAREHP) of high-speed railway in high intensity seismic regions and ensure the repairability of the pier after earthquake. A low yield point steel connection buckle (LYPSCB), which is easy to be installed and to be replaced after earthquake damage, was proposed as a new seismic absorption measure for the pier, and the seismic absorption effect of the LYPSCB was deeply studied. Firstly, the nonlinear numerical model of the SAREHP with energy dissipation bar (SAREHP-EDB) was established according to the pseudo-static test results of the pier completed. Based on the numerical model of the SAREHP-EDB, the SAREHP with the LYPSCB (SAREHP-LYPSCB) was established and corrected. Subsequently, the influence of the LYPSCB on the hysteretic behavior of the SAREHP was studied, and the hysteretic behavior of the SAREHP-LYPSCB was comprehensively compared with a reference to the SAREHP-EDB. Furthermore, considering the far-field seismic wave and the near-field seismic wave with or without pulse, the seismic absorption effect of the LYPSCB was revealed through dynamic time history analysis method. The research results indicated that, by increasing the section contribution rate of the LYPSCB, the horizontal resistance, loading and unloading stiffness as well as energy dissipation capacity of the SAREHP-LYPSCB are significantly improved. However, the residual displacement of the pier is also indirectly increased. Therefore, it is suggested that the section contribution rate of the LYPSCB is controlled and designed in combination with the seismic target displacement and self-centering capacity demand of pier. The hysteretic behavior of the SAREHP-LYPSCB is better than that of the SAREHP-EDB, which indicated that the LYPSCB possesses better seismic absorption effect. Note that the seismic absorption effect of the LYPSCB is more obvious in resisting strong earthquake, in which the seismic absorption rate can reach 80 %. The near-field pulse seismic wave has the greatest impact on the seismic response of the SAREHP-LYPSCB compared with other types of seismic wave, which should be paid special attention.

Keywords: SAREHP, LYPSCB, hysteretic performance, energy dissipation, seismic absorption, seismic wave.

1. Introduction

The poor seismic performance of segmental assembled piers limited its application in high intensity seismic regions. Thus, seismic absorption measures have been proposed by scholars to improve seismic performance and seismic safety of segmental assembled piers. In 2002, Hewes [1] added steel sleeves with different thicknesses and stirrups in the plastic hinge zone to optimize the seismic performance of post-tensioned unbonded prestressed segmental precast assembled piers. The research results showed that the ductility of piers with steel sleeves or stirrups was significantly improved, while the concrete protective layer was obviously cracked. In 2006,

Chung-Che Chou [2] added a metal brace energy dissipation device to the plastic hinge zone of the pier, which has increased lateral restraint, limited the rotation, and reduced the length of the hinge zone, thus improved the energy dissipation capacity of the prestressed connected assembled pier. In 2008, Jui-Chen Wang [3] conducted pseudo-static loading tests on four large-scale precast segmental concrete piers. It was found that adding bonded mild steel reinforcing bars across the segment joints, strengthening the joint at the base of the pier and increasing the height of the base segment can improve the energy dissipation capacity and lateral strength as well as the ductility level of the prestressed connected assembled pier. In 2010, to improve the hysteretic performance and energy dissipation capacity of segmental assembled piers, super elastic shape memory alloy (SMA) reinforcement was set in piers by Hwasung Roh [4]. The research found that SMA reinforcement can not only improve the energy dissipation capacity of precast segmental assembled piers, but also enhance the self-centering capacity and ductility performance of piers. In 2013, Tan Zhen [5] proposed to add viscoelastic dampers outside the prestressed connected assembled pier to reduce its displacement response and improve its self-centering ability. In 2017, Jia Junfeng [6] studied the lateral mechanical behavior of the post-tensioned segmental assembled concrete-filled steel tube (CFST) piers and the seismic performance of bolted precast assembled CFST piers [7]. For the precast segmental CFST piers, the bottom joint opening of the pier was large, and a small amount of concrete was crushed. However, the adjacent joint opening was small. The joint did not have obvious shear dislocation phenomenon, but the steel pipe locally yields, and the pier column has double plastic hinge effect. Thus, it is recommended to set energy dissipation devices at the joint openings to remedy the pier's poor energy dissipation capacity. For the bolt connected precast assembled CFST pier, the horizontal bearing capacity, energy dissipation capacity, and ductility performance were good. The joint opening between segments can be uniformed and the strength of each segment of the pier can be fully used by the reasonable design of the connecting steel pipe size. In the same year, Ehsan Nikbakht [8] researched the influence laws of mild steel ratio on energy dissipation capacity of the self-centering segmental columns with different aspect ratio. In 2018, Wang Zhen [9]-[19] used ultra-high performance concrete material with high strength, high ductility and high durability to reduce the damage at the toe of the segmental assembled pier and improve the energy dissipation capacity. Additionally, the rapid recovery of the pier function after earthquake was achieved through reasonable structural measures. Also in 2018, Jiang Mengying [20] found that the horizontal bearing capacity and energy dissipation capacity of the segmental assembled pier connected by flange were improved, which result in the well improvement of the pier's insufficient energy dissipation. In 2019, Cai Zhong-Kui [21]-[26] proposed a new type of hybrid reinforced precast segmental bridge columns (HR-PSBC), which used common and high-strength mixed reinforcement and has improved the seismic performance of PSBC. The research results showed that HR-PSBC mixed reinforcement is very effective in improving the post-yield stiffness, self-centering capacity, ductility and bearing capacity of the pier. In the same year, Zhuo Wei-Ding [27]-[31] optimized joint connection and improved the seismic performance of precast segmental bridge piers by using high-strength bars. And Zhang Yuye [32] found that compared with the precast segmental bridge columns, the hybrid bridge column made of precast segments and cast-in-place column base have better performance in terms of hysteretic characteristics and energy dissipation. Later, in 2020, Zhang Yuye [33] conducted pseudo-static loading tests on precast segmental bridge columns to study the repair effect of carbon fiber reinforced polymer sheets and sticky steel glue on damaged pier specimens. The results indicated that the rapid repair scheme of carbon fiber reinforced polymer wrapping and sticky steel glue can restore or improve the pier's damage resistance, lateral strength and energy dissipation capacity. To balance the residual drift and the concrete damage zone of precast segmental bridge piers, Teng Tong [34] optimized the hybrid design of high-strength bars and unbonded prestressing tendons. In 2021, Jiang Hui [35] used external self-centering energy dissipation device to improve the energy dissipation and self-centering capacity of precast segmental bridge piers. To mending the inadequate seismic performance and improve the seismic safety of precast segmental assembled pier, a self-centering mortise-tenon segmental bridge pier

was proposed by Yongjun Ni [36].

To sum up, a great number of in-depth studies on seismic absorption measures of precast segmental assembled piers to improve its seismic performance have been conducted in recent years. However, no paper has been published on the seismic mitigation of the SAREHP of high-speed railway proposed in this study, which increases the seismic safety uncertainty of its application in high seismic regions. Therefore, to ensure the seismic safety of high-speed railway bridges, the seismic absorption measure of the SAREHP is in urgent need to be systematically and deeply researched. When the SAREHP is applicated in high-speed railway for seismic absorption, the EDB, simple in structure and design, is often selected and generally embedded in the pier, but it is not convenient to be disassembled and replaced after earthquake, so LYPSCB is proposed in this paper, as a new seismic absorption measure of the SAREHP, it is easy to be installed and replaced. While adopting new seismic absorption measure to improve the hysteretic performance of piers, the self-centering performance of piers will also be affected [37]. The residual displacement angle of piers post-earthquake is the key factor that affects the damage repairment [38], so to control it in this study, the residual displacement angle 1 % is selected as the category of whether pier is easy to be repaired or repairable, and 1.75 % as the category of repairable and difficult to be repaired. Based on this, applying LYPSCB to improve the seismic safety of SAREHP while ensuring its self-resetting ability is deeply studied in this research.

2. Simulation of the SAREHP-EDB

The pseudo-static test results of the SAREHP-EDB completed by our research group was used to correct the numerical model of the pier [39].

2.1. Existing pseudo-static test results of the SAREHP-EDB

The pier test model used in this research was a scale model of a typical precast assembled pier of high-speed railway. The concrete used in the test model is C40. Eighteen HRB400 reinforcements with a diameter of 12 mm were used as the longitudinal tensioned reinforcement. Eight HRB400 bars with a diameter of 25 mm were used as the energy dissipation bars. The prestress provided by prestressed reinforcements is 354 kN, and the axial compression ratio is 7.5 %. The pier is presented in Fig. 1, and the pseudo-static test results is illustrated in Fig. 2.

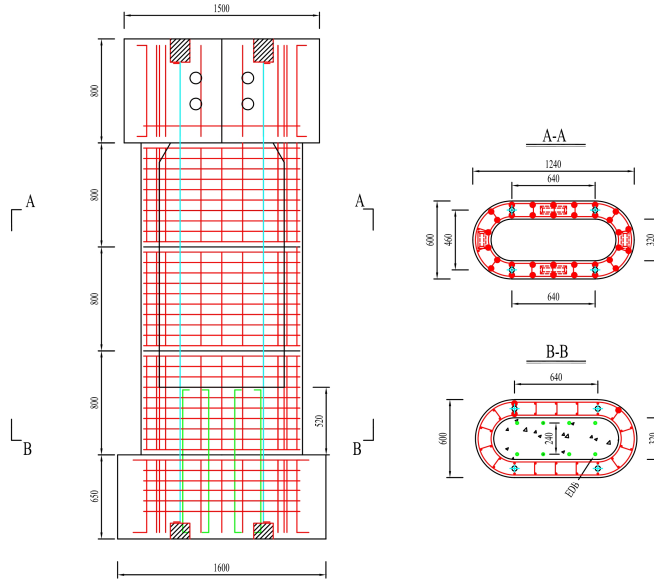

Fig. 1. Structural diagram of the SAREHP-EDB

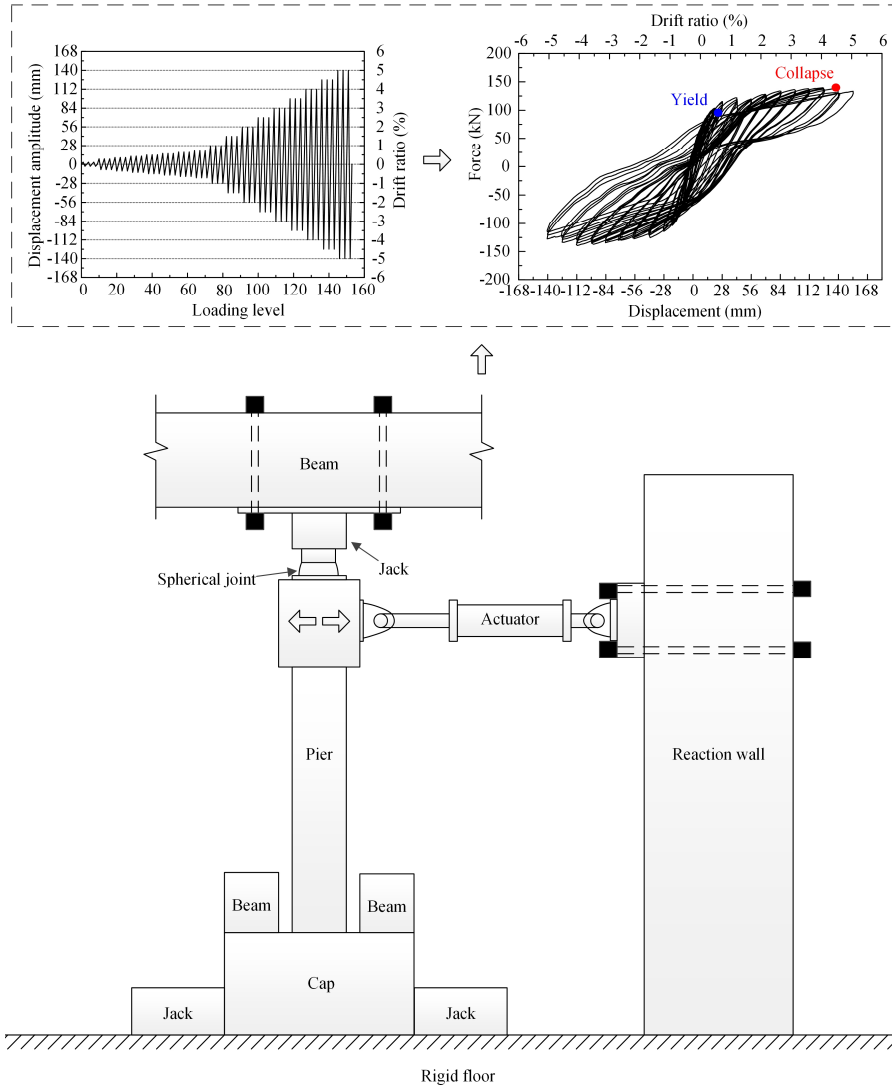

Fig. 2. Pseudo-static test of the SAREHP-EDB

2.2. Numerical simulation method of the SAREHP-EDB

The nonlinear numerical model of the SAREHP-EDB was established by using OpenSees finite element software. When modeling, concrete01 material was used in both the concrete cover and core area of the pier section, and the restraint effect of stirrups on the core area of concrete was considered. Steel 02 material was used for simulation of the longitudinal reinforcement, bonded section and unbonded section of the EDB. The bonded section of the EDB has a length of 320 mm, EDB fiber could be established at the corresponding position of fiber section when modeling. The unbonded section of the EDB has a length of 200 mm, which was simulated by Truss element with its bottom fixed. The detailed pier numerical simulation method and correction results are presented in Fig. 3. It is evident that the simulated cyclic response correlated well with the test results, which indicated that the nonlinear mechanical behavior of the SAREHP-EDB can be accurately reflected by the numerical simulation method.

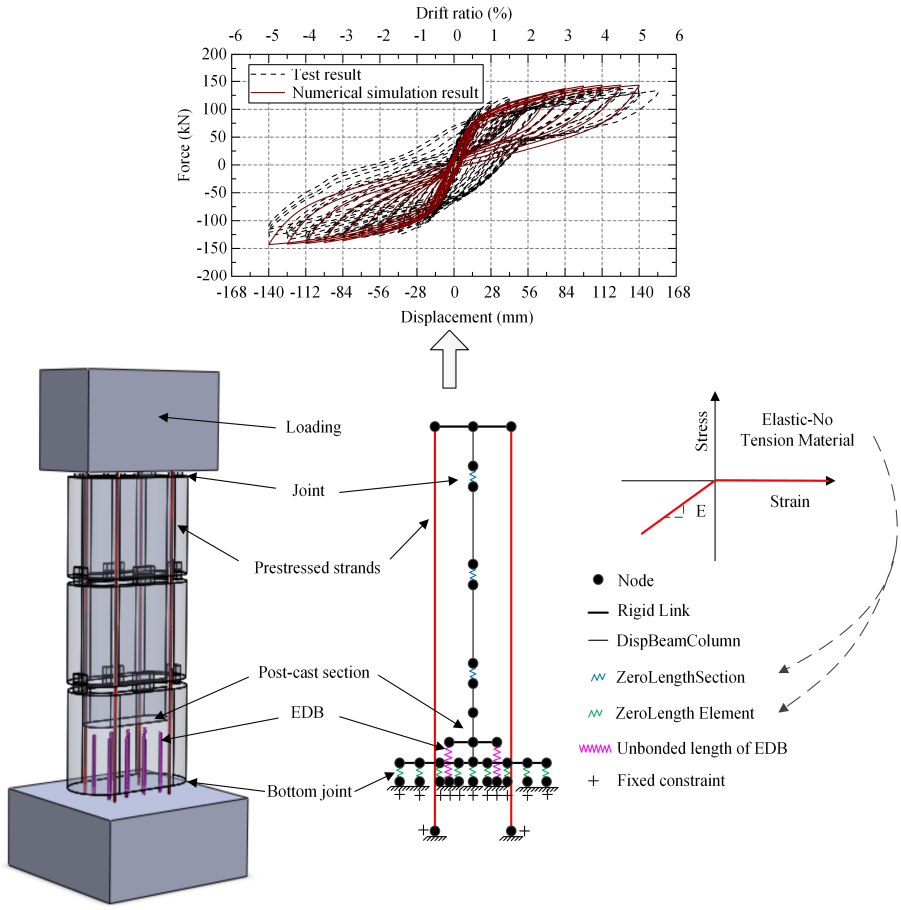

Fig. 3. Numerical simulation method of the SAREHP-EDB

3. Influence of the LYPSCB on hysteretic behavior of the SAREHP-LYPSCB

As EDB is generally embedded in the post-cast section of the SAREHP- EDB, it is not easy to replace the damaged EDB after earthquake. Consequently, it is not conducive to the rapid repair of the pier post-earthquake and causes economic losses to practical application in engineering construction. Therefore, the LYPSCB was proposed in this paper (Fig. 4).

3.1. Service principle and characteristics of the LYPSCB

The energy dissipation principle of the LYPSCB is as follows: The LYPSCB is generally installed at the joint between the bottom segment and the cap of the SAREHP-LYPSCB (Fig. 4). The SAREHP swings while the bottom joint opens and closes continuously under the effect of earthquake, the LYPSCB will work to restrict the movement of joint. The LYPSCB is made of low yield steel, which is prone to plastic deformation. When the SAREHP-LYPSCB swings, the LYPSCB will deform synchronously with the swing behavior of the pier. When a small earthquake occurs, the swing of the pier and the motion amplitude of the joint are small. The LYPSCB is in the elastic deformation stage, which can not only restraint the swing behavior of the SAREHP-LYPSCB and the displacement of the pier top, but also provide a certain self-centering effect to the pier and the joint. During a strong earthquake, the swing of the pier and the motion amplitude of the joint position increase, which prompting the LYPSCB to enter plastic deformation and begin to exert its own energy dissipation effect by dissipating the energy that the

earthquake puts into the SAREHP-LYPSCB and reducing the displacement of the SAREHP-LYPSCB top.

The size, quantity, and installation location of the LYPSCB can be designed according to the actual engineering demands. This LYPSCB is simple in structure, low in cost, easy to be installed and replaced, and feasible for standardized and industrialized production. Compared with the EDB, the damaged LYPSCB can be replaced quickly and the SAREHP-LYPSCB can also be quickly repaired after earthquake, which significantly reduce the economic loss of engineering construction.

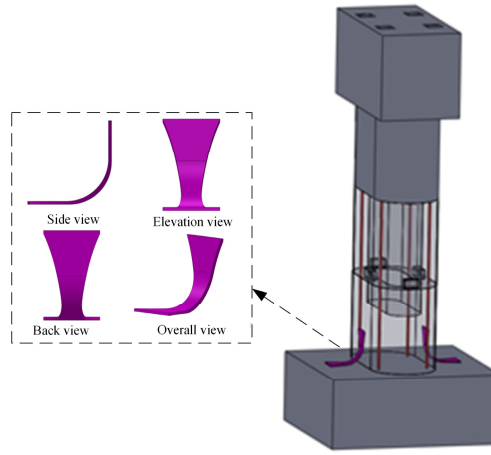

Fig. 4. Structural diagram of the LYPSCB

3.2. Modeling of the LYPSCB

The detailed modeling method of the LYPSCB is illustrated in Fig. 5.

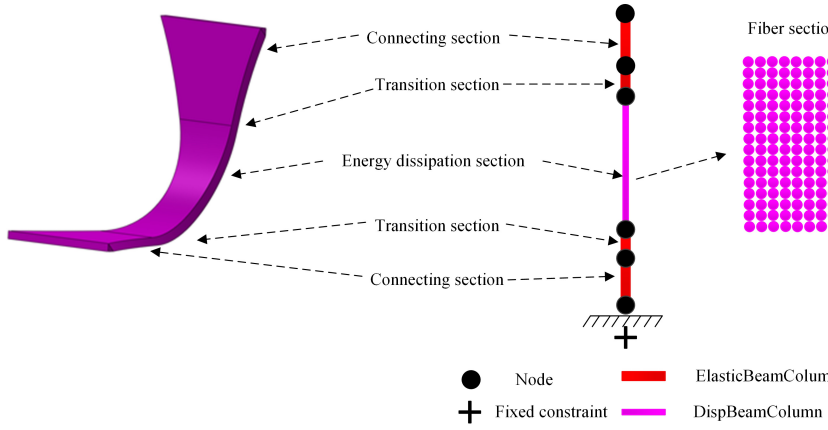

Fig. 5. Modeling of the LYPSCB

3.3. The influence of the LYPSCB on the hysteretic behavior of the SAREHP-LYPSCB

The LYPSCB numerical model and the pier fiber model was connected by rigid arms. The modeling method of the pier adopted the numerical simulation method given above. Then the influence of the LYPSCB design parameters on the hysteretic behavior of the SAREHP-LYPSCB was studied.

3.4. The hysteretic behavior of the SAREHP-LYPSCB with the LYPSCB arrangement 1

The area of energy dissipation section of the LYPSCB, mainly determined by the section's length and width, is an important design parameter that affects the seismic performance of the SAREHP-LYPSCB. LYPSCB was installed at the front and back of the pier along the bridge longitudinal direction (as presented in Fig. 6) to give full play of its seismic absorption effect. The energy dissipation section of the LYPSCB along the bridge longitudinal direction should be the weak axis to ensure it undergoes the plastic deformation and to exert its energy dissipation effect. Therefore, the section width of the energy dissipation section of the LYPSCB was kept at 20 mm while the section length ranges from 20 mm to 100 mm with an interval of 10 mm between each section, as presented in Table 1.

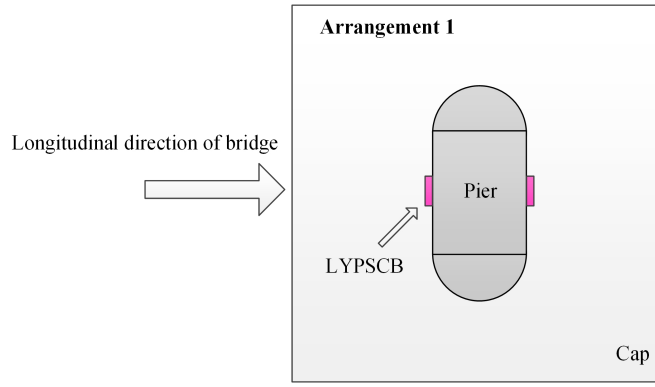

Fig. 6. Arrangement 1 of the LYPSCB

Table 1. Changing of the section contribution rate of the LYPSCB

Model	Length (mm)	Width (mm)	Area (mm^2)	Area of arrangement 1 (mm^2)	Section contribution rate (%)
SAREHP-LYPSCB 1	20	20	400	800	0.12
SAREHP-LYPSCB 2	30	20	600	1200	0.18
SAREHP-LYPSCB 3	40	20	800	1600	0.24
SAREHP-LYPSCB 4	50	20	1000	2000	0.30
SAREHP-LYPSCB 5	60	20	1200	2400	0.36
SAREHP-LYPSCB 6	70	20	1400	2800	0.42
SAREHP-LYPSCB 7	80	20	1600	3200	0.48
SAREHP-LYPSCB 8	90	20	1800	3600	0.54
SAREHP-LYPSCB 9	100	20	2000	4000	0.60

Based on the above numerical simulation method of the SAREHP-LYPSCB, the corresponding numerical models were established and hysteretic analyzed was carried out on OpenSees platform, as presented in Fig. 7.

By analyzing the data in Fig. 7(a) and (b), it showed that the maximum horizontal resistance of the SAREHP-LYPSCB 1 is 110.69 kN, and that of the SAREHP-LYPSCB 9 is 212.25 kN. The corresponding section contribution rate changes from 0.12 % to 0.6 %, which indirectly leads to the horizontal resistance changes to 1.92 times of the original one. It revealed that the larger the section area of the LYPSCB energy dissipation section, the higher the horizontal resistance of the LYPSCB, which indirectly improve the horizontal bearing capacity of the SAREHP-LYPSCB. According to the analysis of Fig. 7(c), the maximum residual displacement of the SAREHP-LYPSCB 1 is 4.67 mm, and that of the SAREHP-LYPSCB 9 is 90.31 mm, which indicated that the residual displacement changes to 19.34 times of the original one. It is evident that under the same loading displacement amplitude, the degree of plastic deformation of the LYPSCB increases as the area of the energy dissipation section becoming larger, which indirectly

leads to the increase of residual deformation of the SAREHP-LYPSCB after swings. Moreover, the residual displacement angle of the SAREHP-LYPSCB 5 to SAREHP-LYPSCB 9 exceeds 1 %, and that of the SAREHP-LYPSCB 7 to SAREHP-LYPSCB 9 even exceeds1.75 %. It's worth noting that the residual displacement angle of the SAREHP-LYPSCB 9 exceeds 1.75 % when its loading displacement amplitude reaches 84 mm.

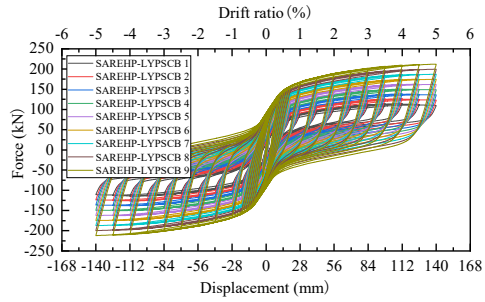

a) Hysteresis curves

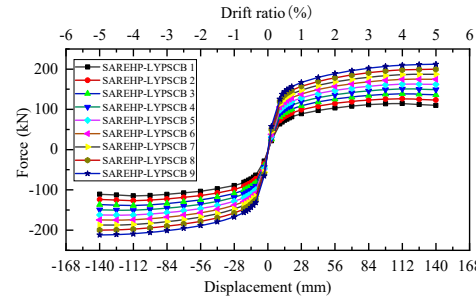

b) Skeleton curves

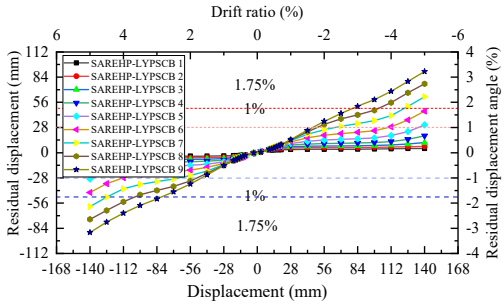

c) Residual displacement

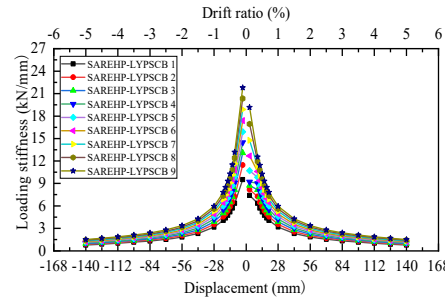

d) Loading stiffness

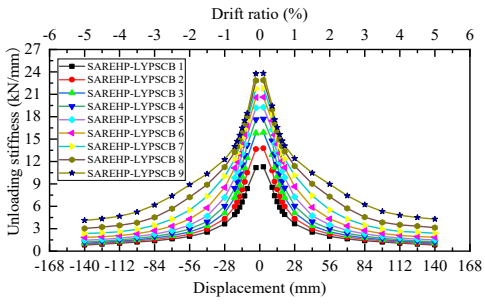

e) Unloading stiffness

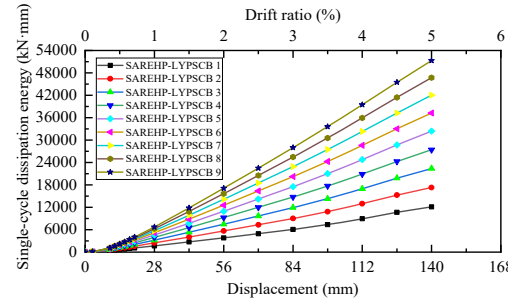

f) Hysteretic energy dissipation

Fig. 7. Hysteretic behavior of the SAREHP with the LYPSCB arrangement 1

The analysis result of Fig. 7(d) and (e) shows that the force required for unit deformation of each LYPSCB rises with the increase of the energy dissipation section area of the LYPSCB, consequently, the force for unit deformation of the SAREHP-LYPSCB also climbs. The maximum loading stiffness of the SAREHP-LYPSCB 1 is 9.52 kN/mm, that of the SAREHP-LYPSCB 9 is 21.79 kN/mm, so the loading stiffness changes to 2.29 times of the original one. The maximum unloading stiffness of the SAREHP-LYPSCB 1 is 11.29 kN/mm, and that of the SAREHP-LYPSCB 9 is 23.81 kN/mm, so the unloading stiffness changes to 2.11 times of the original one.

In Fig. 7(f), under the same loading displacement amplitude, the LYPSCB with a large energy dissipation section area shows a larger degree of plastic deformation and stronger energy

dissipation capacity, so the corresponding SAREHP-LYPSCB possesses a larger energy dissipation capacity. The maximum single-cycle dissipation energy of the SAREHP-LYPSCB 1 is 12129.15 kN·mm, that of the SAREHP-LYPSCB 9 is 51290.21 kN·mm, so the maximum single-cycle energy dissipation changes to 4.23 times of the original one.

3.5. The hysteretic behavior of the SAREHP-LYPSCB with the LYPSCB arrangement 2

To conduct further study the influence of LYPSCB installation position on the hysteretic performance of the SAREHP-LYPSCB, the LYPSCB was installed on each side of the pier (as presented in Fig. 8).

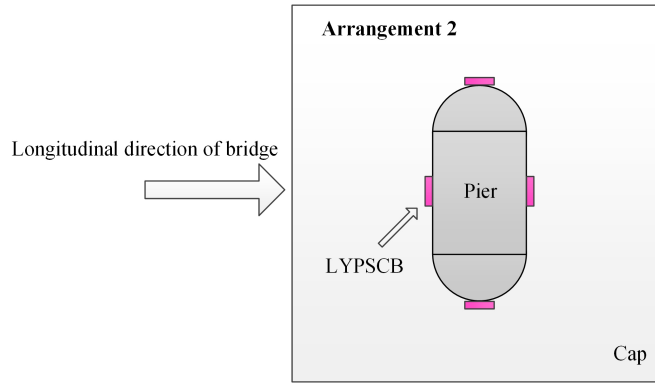

Fig. 8. Arrangement 2 of the LYPSCB

Table 2. Changing of the section contribution rate of the LYPSCB

Model	Length (mm)	Width (mm)	Area (mm^2)	Area of arrangement 2 (mm^2)	Section contribution rate (%)
SAREHP-LYPSCB 10	20	20	400	1600	0.24
SAREHP-LYPSCB 11	30	20	600	2400	0.36
SAREHP-LYPSCB 12	40	20	800	3200	0.48
SAREHP-LYPSCB 13	50	20	1000	4000	0.60
SAREHP-LYPSCB 14	60	20	1200	4800	0.72
SAREHP-LYPSCB 15	70	20	1400	5600	0.84
SAREHP-LYPSCB 16	80	20	1600	6400	0.96
SAREHP-LYPSCB 17	90	20	1800	7200	1.08
SAREHP-LYPSCB 18	100	20	2000	8000	1.20

The width of the LYPSCB energy dissipation section kept unchanged, and length of its energy dissipation section was increased with a variation range of 20-100 mm and an interval of 10 mm, as presented in Table 2.

The corresponding numerical models were established and analyzed by OpenSees platform, as presented in Fig. 9.

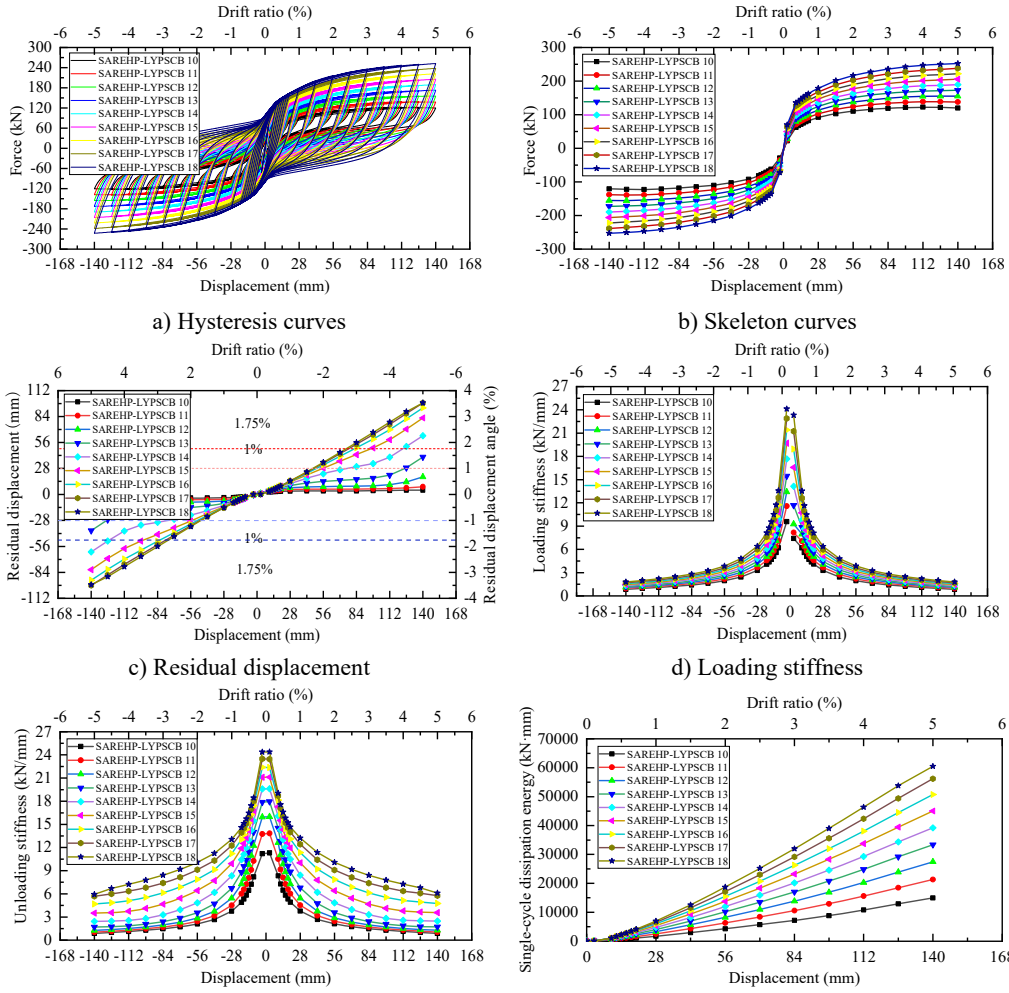

Fig. 9. Hysteretic behavior of the SAREHP-LYPSCB with the LYPSCB arrangement 2

By analyzing Fig. 9 (a) and (b), the maximum horizontal resistance of the SAREHP-LYPSCB 10 is 120.39 kN, and that of the SAREHP-LYPSCB 18 is 252.86 kN, which indicated that the horizontal resistance changes to 2.10 times of the original one.

According to the analysis of Fig. 9(c), the maximum residual displacement of the SAREHP-LYPSCB 10 is 3.95 mm, 98.69 mm for the SAREHP-LYPSCB 18, so the residual displacement changes to 24.98 times of the original one. Moreover, the residual displacement angle of the SAREHP-LYPSCB 13 to SAREHP-LYPSCB 18 exceeds 1 %, and that of the SAREHP-LYPSCB 14 to SAREHP-LYPSCB 18 even exceeds 1.75 %. The residual displacement angle of the SAREHP-LYPSCB 18 exceeds 1.75 % when its loading displacement amplitude reaches 84 mm.

The analysis results of Fig. 9(d) and (e) show that the loading and unloading stiffness of the SAREHP-LYPSCB increases with increasing of the area of the energy dissipation section of the LYPSCB. The maximum loading stiffness of the SAREHP-LYPSCB 10 is 9.57 kN/mm, that of the SAREHP-LYPSCB 18 is 24.13 kN/mm, so the loading stiffness changes to 2.52 times of the original one. The maximum unloading stiffness of the SAREHP-LYPSCB 10 is 11.31 kN/mm, that of the SAREHP-LYPSCB 18 is 24.39 kN/mm, so the unloading stiffness changes to 2.16

times of the original one.

In Fig. 9(f), the maximum single-cycle dissipation energy of the SAREHP-LYPSCB 10 is 14976.96 kN·mm, that of the SAREHP-LYPSCB 18 is 60505.18 kN·mm, which indicated that the maximum single-cycle dissipation energy changes to 4.04 times of original one.

3.6. Comparative research on hysteretic behavior of the piers with different seismic absorption measures

To further verify the seismic absorption effect of the LYPSCB, comparative research on the hysteretic performance of the SAREHP-EDB (the section contribution rate of the EDB was 0.59 %) and the SAREHP-LYPSCB 4 (the section contribution rate of the LYPSCB was 0.3 %) was carried out, as presented in Fig. 10.

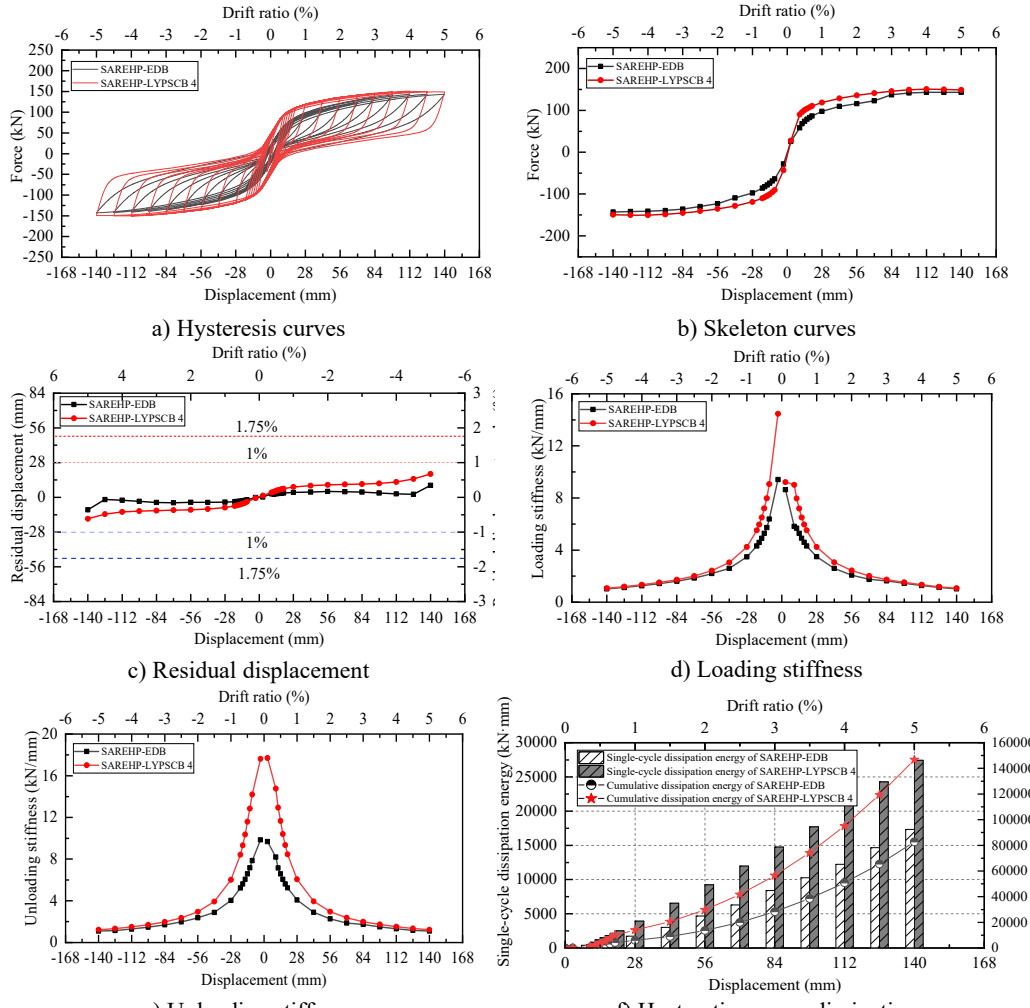

Fig. 10. Comparison of hysteretic behavior between the SAREHP-EDB and the SAREHP-LYPSCB 4

Fig. 10(a) shows that the hysteresis curve of SAREHP-EDB was completely covered by SAREHP-LYPSCB 4. Fig. 10(b) shows that the maximum horizontal resistance of the SAREHP-EDB is 143.26 kN, that of the SAREHP-LYPSCB 4 is 149.29 kN, so the maximum horizontal resistance of the SAREHP-LYPSCB 4 is 4.2 % higher than the SAREHP-EDB.

Fig. 10(c) shows that the maximum residual displacement of the SAREHP-EDB is 9.97 mm, that of the SAREHP-LYPSCB 4 is 18.77 mm, so the maximum residual displacement of the SAREHP-LYPSCB 4 is 1.88 times of the SAREHP-EDB, but neither of them exceeds the limited residual displacement angle of 1 %. According to Fig. 10(d) and (e), the maximum loading stiffness of the SAREHP-EDB is 9.42 kN/mm, the SAREHP-LYPSCB 4 is 14.46 kN/mm, so the maximum loading stiffness of the SAREHP-LYPSCB 4 is 1.54 times of the SAREHP-EDB. The maximum unloading stiffness of the SAREHP-EDB is 9.84 kN/mm, the SAREHP-LYPSCB 4 is 17.70 kN/mm, so the maximum unloading stiffness the SAREHP-LYPSCB 4 is 1.80 times of the SAREHP-EDB. Fig. 10(f) shows that the maximum single-cycle dissipation energy of the SAREHP-EDB and the SAREHP-LYPSCB 4 are respectively 17321.4 kN·mm 1 and 27432.78 kN·mm, the maximum cumulative dissipation energy is 82725.97 kN·mm for the former and 146767.71 kN·mm for the latter, so the maximum single-cycle dissipation energy of the SAREHP-LYPSCB 4 is 1.58 times of the SAREHP-EDB, and the maximum cumulative dissipation energy of the SAREHP-LYPSCB 4 is 1.77 times of the SAREHP-EDB.

To sum up, the hysteretic performance of the SAREHP-LYPSCB is better than the SAREHP-EDB. It is feasible to replace EDB with LYPSCB in the seismic design of the SAREHP.

4. Research on seismic absorption effect of the LYPSCB based on dynamic time history analysis method

With the SAREHP without seismic absorption measure and the SAREHP-EDB (the section contribution rate of energy dissipation bar 0.59 %) taking as references, the seismic absorption effect of the LYPSCB on the SAREHP-LYPSCB was studied. Among them, the SAREHP-LYPSCB 4 with good hysteretic performance (the section contribution rate of the energy dissipation section of the LYPSCB was 0.3 %) was selected as the pier model that applied the LYPSCB seismic absorption technology.

4.1. Selection of seismic wave

Thirty seismic waves (Fig. 11) were selected from the PEER database, including 10 near-field pulse seismic waves, 10 near-field no-pulse seismic waves and 10 far-field seismic waves.

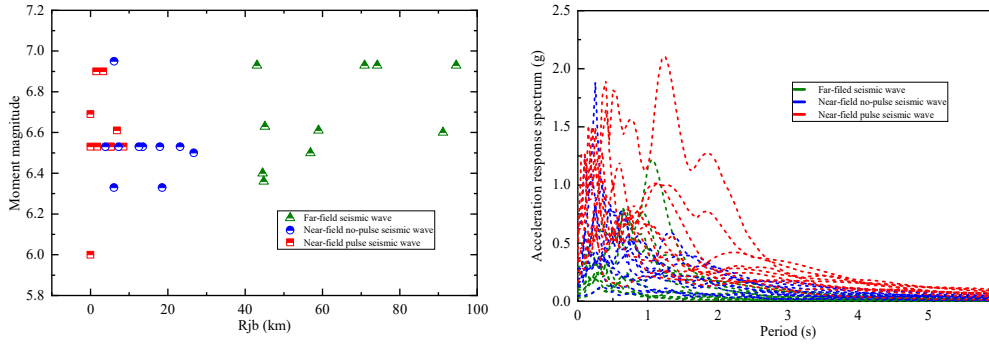

a) Seismic waves b) Response spectrum

Fig. 11. Thirty records of seismic waves

The fault distance of near-field seismic waves was 0-30 km, 30-100 km for far-field seismic waves, and the duration of velocity pulse of near-field pulse seismic wave was larger than 1 s. Subsequently, the selected seismic waves were normalized, and then the peak acceleration amplitude of each seismic wave was adjusted to the range of 0.2 g-1.0 g with an interval of 0.2 g, which was then successively input into the numerical model of the piers for dynamic time history analysis.

4.2. Comparative research of seismic response of the piers

Taking RSN 69 far-field seismic wave (peak acceleration adjusted to 0.2 g) and RSN 1114 near-field pulse seismic wave (peak acceleration adjusted to 1.0 g) as examples, the calculation results are illustrated in Fig. 12.

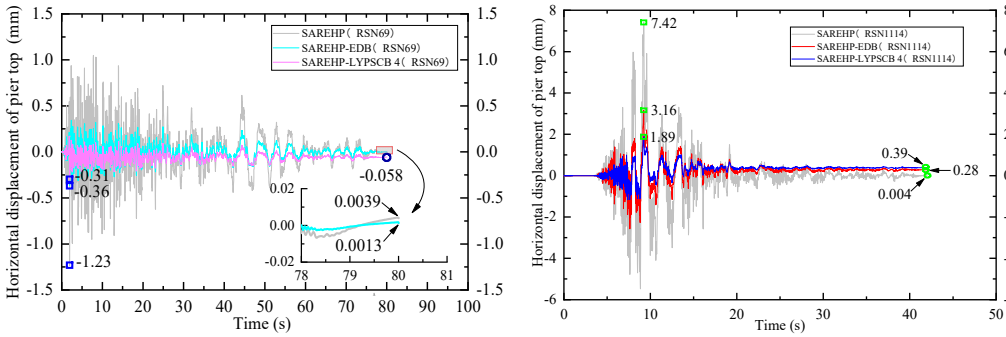

a) RSN69 b) RSN1114

Fig. 12. Comparative of seismic response of the piers

According to Fig. 12(a), under the action of RSN 69 seismic wave (peak acceleration of 0.2 g), the seismic absorption rate of the SAREHP-EDB is 71 %, and that of the SAREHP-LYPSCB 4 is 75 %. The residual displacement of the SAREHP-EDB is 0.0026 mm smaller than the SAREHP, while the SAREHP-LYPSCB 4 is 0.0541mm larger than the SAREHP. Fig. 12(b) shows that under the action of RSN1114 seismic wave (peak acceleration of 1.0 g), the seismic absorption rate of the SAREHP-EDB is 57 %, and that of the SAREHP-LYPSCB 4 is 75 %. The residual displacement of the SAREHP-EDB is 0.276 mm larger than the SAREHP, and the residual displacement of SAREHP-LYPSCB 4 is 0.386 mm larger than the SAREHP. It indicates that when small earthquake occurs, the EDB not only reduces the displacement response of the pier top, but also provides a certain self-centering capacity. Compared with the EDB set inside the pier, LYPSCB shows earlier plastic deformation, better seismic absorption effect and increases the residual displacement of the pier post-earthquake. Under the impact of large earthquake, the plastic deformation of the LYPSCB is larger than the EDB, which indicates that the seismic absorption effect of the SAREHP-LYPSCB 4 is obviously better than that of the SAREHP-EDB. It is also found that the residual displacement of the SAREHP-LYPSCB 4 is larger than the SAREHP-EDB, but the residual displacement values of the piers are small, which exert no influence on the repair of the piers post-earthquake.

To further research the seismic absorption capacity of the LYPSCB, the difference between the mean value of maximum displacement and residual displacement of pier top under different types of seismic waves was compared, as presented in Fig. 13.

By analyzing Fig. 13, the result shows that under the impact of seismic wave, the seismic absorption effect of the SAREHP-LYPSCB 4 is better than the SAREHP-EDB. The amplitude of displacement response at the pier top decreases obviously as the seismic peak acceleration increases. For example, when the seismic peak acceleration of near-field pulse seismic wave is 0.2 g, the displacement response at the pier top of the SAREHP-EDB is 1.34 mm smaller than the SAREHP, and the seismic absorption rate of the SAREHP-EDB is 69 %. The displacement response at the pier top of the SAREHP-LYPSCB 4 is 1.57 mm smaller than the SAREHP, and the seismic absorption rate of the SAREHP-LYPSCB 4 is 81 %. When the seismic peak acceleration of near-field pulse seismic wave is 1.0 g, the displacement response at the pier top of the SAREHP-EDB is 6.71 mm smaller than the SAREHP, and the seismic absorption rate of the SAREHP-EDB is 68 %. The displacement response at the pier top of the SAREHP-LYPSCB 4 is 7.99 mm smaller than the SAREHP, and the seismic absorption rate of the SAREHP-LYPSCB 4

is 81 %. The main reason for this result is that, compared with the EDB, the LYPSCB is Q235 steel with low yield point and is installed outside the pier, thus, the LYPSCB shows earlier plastic deformation and dissipates the energy the seismic wave input to the pier. In addition, compared with the far-field seismic wave, the LYPSCB has a better seismic absorption effect under the near-field seismic wave. For example, when the seismic peak acceleration is 1.0 g, the seismic absorption rate of the SAREHP-LYPSCB 4 under the far-field seismic wave is 78 %, the SAREHP-LYPSCB 4 under the near-field no-pulse seismic wave is 83 %, and the SAREHP-LYPSCB 4 under the near-field pulse seismic wave is 81 %. The near-field effect of seismic wave is the main reason for this result, under the effect of which, the pier shows larger displacement response, which the plastic state of LYPSCB continues to deepen to better exert its seismic absorption effect by dissipating more energy input by earthquake.

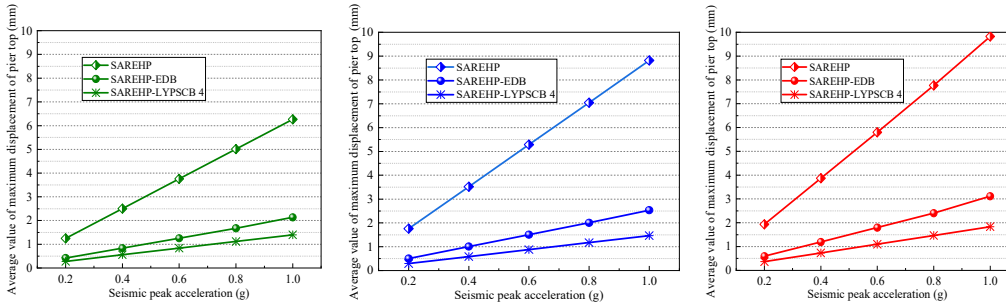

a) Far-field seismic wave b) Near-field no-pulse seismic wave c) Near-field pulse seismic wave

Fig. 13. Average value of maximum displacement of the piers tops under different types of seismic waves

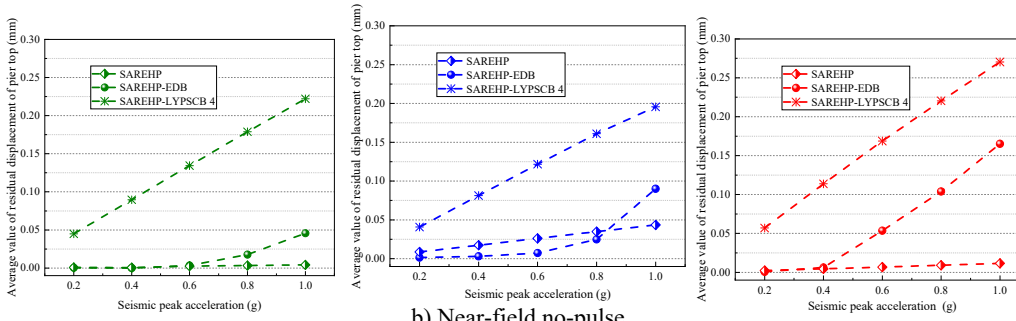

a) Far-field seismic wave b) Near-field no-pulse seismic wave c) Near-field pulse seismic wave

Fig. 14. Average value of residual displacement of the piers under different types of seismic waves

Fig. 14 shows that, under the influence of three types of seismic waves, the SAREHP-LYPSCB 4's average residual displacement value is larger than that of the SAREHP and the SAREHP-EDB. Besides, under the action of different seismic peak accelerations, the law is basically consistent. The results can be explained as that the LYPSCB undergoes plastic deformation in resisting the action of seismic waves, which indirectly increases the residual displacement of the pier. Thus, the residual displacement of the SAREHP-LYPSCB 4 is much larger than that of the SAREHP. In addition, by installing outside the pier, the LYPSCB is easier to enter the plastic state than the EDB built-in the pier, which produces larger unrecoverable deformation, which resulting in the larger residual displacement of the SAREHP-LYPSCB 4. But all residual displacement values of the piers are small, which will not affect the repair of the piers post-earthquake at all.

4.3. Influence of different types of earthquakes on the SAREHP-LYPSCB

Further, the influence of different types of seismic waves on the SAREHP-LYPSCB was

studied, as presented in Fig. 15.

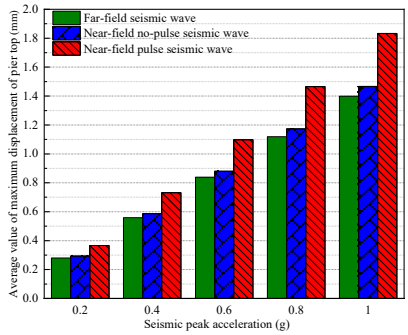

a) Average value of maximum displacement of the pier top

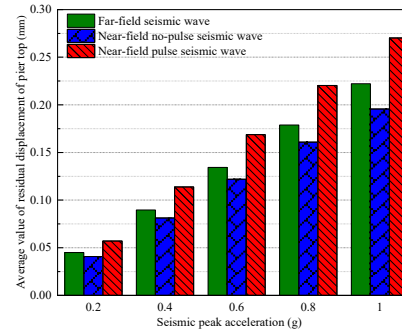

b) Average value of residual displacement of the pier top

Fig. 15. The influence of different types of seismic waves on the SAREHP-LYPSCB

In Fig. 15(a), the maximum average pier top displacement value of the SAREHP-LYPSCB 4 under the effect of the near-field pulse seismic wave is greater than that under the near-field no-pulse seismic wave. The former two are greater than the maximum average displacement value under the effect of the far-field pulse seismic wave. Additionally, the difference is even more obvious with the growing of the peak acceleration of seismic wave. For example, when the seismic peak acceleration is 0.2 g, the maximum average pier top displacement value under the influence of the near-field pulse seismic wave is 0.0864 mm larger than the value under the influence of the far-field seismic wave. When the seismic peak acceleration is 1.0 g, the maximum average displacement value of the pier top under the influence of the near-field pulse seismic wave is 0.43 mm larger than the far-field seismic wave.

In Fig. 15(b), although the average pier top residual displacement value of the SAREHP-LYPSCB 4 under the action of the far-field seismic wave is larger than the near-field no-pulse seismic wave, the residual displacement of the SAREHP-LYPSCB 4 pier top under the action of near-field pulse seismic wave is the largest. With the rising of peak acceleration of seismic wave, the impact of near-field pulse seismic wave on the SAREHP-LYPSCB 4 becomes more obvious. For example, when the seismic peak acceleration is 0.2 g, the pier top's average value of the residual displacement under the action of the near-field pulse seismic wave is 0.012 mm larger than the far-field seismic wave. When the seismic peak acceleration 1.0 g, the pier top's average value of the residual displacement under the action of the near-field pulse seismic wave is 0.048 mm larger than the far-field seismic wave.

5. Conclusions

The following conclusions can be drawn by conducting research on the seismic absorption of high-speed railway SAREHP-LYPSCB:

1) It will be easier to be cannibalized and replaced after earthquake when the LYPSCB is installed outside the SAREHP. Besides, LYPSCB is made of Q235 steel with low yield point, which prompting its ability to show earlier plastic deformation and to better dissipate the energy input by the seismic wave to the pier. To sum up, LYPSCB shows a good application prospect in improving the seismic safety of the SAREHP.

2) When two sets of LYPSCB installed along the direction of pier, as the section contribution rate of the energy dissipation section gradually grows from 0.12 % to 0.6 %, the SAREHP-LYPSCB's horizontal resistance increased by1.92 times, the loading stiffness increased by 2.29 times, the unloading stiffness increased by 2.11 times, and the energy dissipation of single-cycle increased by 4.23 times. When one set of LYPSCB installed around the pier, as the

section contribution rate of the energy dissipation section consistently rises from 0.24 % to 1.2 %, the SAREHP-LYPSCB's horizontal resistance increased by 2.10 times, the loading stiffness increased by 2.52 times, the unloading stiffness increased by 2.16 times, and the energy dissipation of single-cycle increased by 4.04 times.

3) The hysteretic behavior of the SAREHP-LYPSCB is better than the SAREHP-EDB. In addition, it can be found that the seismic absorption ability of the LYPSCB is more effective in resisting strong earthquake, with its seismic absorption rate reaches 80 %. Therefore, the EDB can be replaced by the LYPSCB to achieve better seismic absorption effect.

4) However, the LYPSCB produces plastic deformation to restrain the opening and closing of joints between pier segments due to the action of earthquake, which indirectly increases the residual displacement of the SAREHP-LYPSCB post-earthquake. Thus, to guarantee the pier's effective damage repair after earthquake, the section contribution rate of the LYPSCB should be controlled based on the seismic target displacement and self-centering capacity demand of pier.

5) Note that the near-field pulse seismic waves show the greatest impact on the seismic response of the SAREHP-LYPSCB than the near-field no-pulse and far-field seismic waves, so special attention shall be paid to the seismic safety of the pier that applied in the near-fault region.

Acknowledgements

This study is sponsored by the special scientific research fund for academician of CCCC (Grant No. YSZX-03-2021-02-B).

Data availability

The datasets generated during and/or analyzed during the current study are available from the corresponding author on reasonable request.

Conflict of interest

The authors declare that they have no conflict of interest.

References

[1] Joshua T. Hewes and M. Priestley, "Seismic design and performance of precast concrete segmental bridge columns," University of California, San Diego, 2002.

[2] C.-C. Chou and Y.-C. Chen, "Cyclic tests of post-tensioned precast CFT segmental bridge columns with unbonded strands," *Earthquake Engineering and Structural Dynamics*, Vol. 35, No. 2, pp. 159–175, Feb. 2006, https://doi.org/10.1002/eqe.512

[3] J.-C. Wang, Y.-C. Ou, K.-C. Chang, and G. C. Lee, "Large-scale seismic tests of tall concrete bridge columns with precast segmental construction," *Earthquake Engineering and Structural Dynamics*, Vol. 37, No. 12, pp. 1449–1465, Oct. 2008, https://doi.org/10.1002/eqe.824

[4] H. Roh and A. M. Reinhorn, "Hysteretic behavior of precast segmental bridge piers with superelastic shape memory alloy bars," *Engineering Structures*, Vol. 32, No. 10, pp. 3394–3403, Oct. 2010, https://doi.org/10.1016/j.engstruct.2010.07.013

[5] Z. Tan, "Seismic performance of post-tensioned precast concrete segmental bridge columns with viscoelastic dampers," (in Chinese), Harbin Institute of technology, 2013.

[6] J. F. Jia et al., "Experimental on lateral bearing behavior of post-tensioned segmental CFST bridge pier columns," *China Journal of Highway and Transport*, Vol. 30, No. 3, pp. 236–245, 2017.

[7] J. F. Jia et al., "Cyclic testing on seismic behavior of precast segmental CFST bridge piers with bolted connections," *China Journal of Highway and Transport*, Vol. 30, No. 12, pp. 242–249, 2017.

[8] E. Nikbakht and K. Rashid, "Investigation on seismic performance and functionality of self-centring post-tensioned segmental columns," *Structure and Infrastructure Engineering*, Vol. 14, No. 6, pp. 730–742, Jun. 2018, https://doi.org/10.1080/15732479.2017.1359632

[9] Z. Wang, "Research on seismic performance and design method of self-centering precast segmental UHPC hollow bridge Piers," (in Chinese), Southeast University, 2018.

[10] Z. Wang, J.-Q. Wang, T.-X. Liu, and J. Zhang, "An explicit analytical model for seismic performance of an unbonded post-tensioned precast segmental rocking hollow pier," *Engineering Structures*, Vol. 161, pp. 176–191, Apr. 2018, https://doi.org/10.1016/j.engstruct.2018.02.025

[11] Z. Wang, J.-Q. Wang, Y.-C. Tang, T.-X. Liu, Y.-F. Gao, and J. Zhang, "Seismic behavior of precast segmental UHPC bridge columns with replaceable external cover plates and internal dissipaters," *Engineering Structures*, Vol. 177, pp. 540–555, Dec. 2018, https://doi.org/10.1016/j.engstruct.2018.10.012

[12] J. Wang, Z. Wang, Y. Tang, T. Liu, and J. Zhang, "Cyclic loading test of self-centering precast segmental unbonded posttensioned UHPFRC bridge columns," *Bulletin of Earthquake Engineering*, Vol. 16, No. 11, pp. 5227–5255, Nov. 2018, https://doi.org/10.1007/s10518-018-0331-y

[13] Z. Wang, J. Wang, Y. Tang, Y. Gao, and J. Zhang, "Lateral behavior of precast segmental UHPC bridge columns based on the equivalent plastic-hinge model," *Journal of Bridge Engineering*, Vol. 24, No. 3, p. 04018124, Mar. 2019, https://doi.org/10.1061/(asce)be.1943-5592.0001332

[14] Z. Wang, J.-Q. Wang, and T.-X. Liu, "Axial compression ratio limit for self-centering precast segmental hollow piers," *Structural Concrete*, Vol. 18, No. 5, pp. 668–679, Oct. 2017, https://doi.org/10.1002/suco.201600152

[15] Z. Wang, J. Wang, T. Liu, and F. Zhang, "Modeling seismic performance of high-strength steel-ultra-high-performance concrete piers with modified Kent-Park model using fiber elements," *Advances in Mechanical Engineering*, Vol. 8, No. 2, p. 168781401663341, Feb. 2016, https://doi.org/10.1177/1687814016633411

[16] T. Liu, Z. Wang, J. Guo, and J. Wang, "Shear strength of dry joints in precast UHPC segmental bridges: Experimental and theoretical research," *Journal of Bridge Engineering*, Vol. 24, No. 1, p. 04018100, Jan. 2019, https://doi.org/10.1061/(asce)be.1943-5592.0001323

[17] Z. Wang, J. Wang, G. Zhao, and J. Zhang, "Design criterion for the self-centering capacity of precast segmental UHPC bridge columns with unbonded post-tensioning tendons," *Engineering Structures*, Vol. 200, p. 109706, Dec. 2019, https://doi.org/10.1016/j.engstruct.2019.109706

[18] Z. Wang, J. Wang, G. Zhao, and J. Zhang, "Modeling seismic behavior of precast segmental UHPC bridge columns in a simplified method," *Bulletin of Earthquake Engineering*, Vol. 18, No. 7, pp. 3317–3349, May 2020, https://doi.org/10.1007/s10518-020-00817-z

[19] Z. Wang, J. Wang, K. Chen, and J. Zhang, "Feasible region of post-tensioning force for precast segmental post-tensioned UHPC bridge columns," *Engineering Structures*, Vol. 200, p. 109685, Dec. 2019, https://doi.org/10.1016/j.engstruct.2019.109685

[20] M. Y. Jiang, "Research and improvement on seismic performance of precast segmental concrete-filled tube bridge piers," (in Chinese), Beijing Jiaotong University, 2018.

[21] Z. K. Cai, "Seismic performance and design method of hybrid reinforced precast segmental bridge columns," (in Chinese), Harbin Institute of technology, 2018.

[22] Z.-K. Cai, Z. Wang, and T. Y. Yang, "Cyclic load tests on precast segmental bridge columns with both steel and basalt FRP reinforcement," *Journal of Composites for Construction*, Vol. 23, No. 3, p. 04019014, Jun. 2019, https://doi.org/10.1061/(asce)cc.1943-5614.0000944

[23] Z.-K. Cai, Z. Wang, and T. Y. Yang, "Experimental testing and modeling of precast segmental bridge columns with hybrid normal – and high-strength steel rebars," *Construction and Building Materials*, Vol. 166, pp. 945–955, Mar. 2018, https://doi.org/10.1016/j.conbuildmat.2018.01.159

[24] Z.-K. Cai, Z. Zhou, and Z. Wang, "Influencing factors of residual drifts of precast segmental bridge columns with energy dissipation bars," *Advances in Structural Engineering*, Vol. 22, No. 1, pp. 126–140, Jan. 2019, https://doi.org/10.1177/1369433218780545

[25] Z.-K. Cai, D. Wang, and Z. Wang, "Full-scale seismic testing of concrete building columns reinforced with both steel and CFRP bars," *Composite Structures*, Vol. 178, pp. 195–209, Oct. 2017, https://doi.org/10.1016/j.compstruct.2017.06.020

[26] Z. Cai, D. Wang, S. T. Smith, and Z. Wang, "Experimental investigation on the seismic performance of GFRP-wrapped thin-walled steel tube confined RC columns," *Engineering Structures*, Vol. 110, pp. 269–280, Mar. 2016, https://doi.org/10.1016/j.engstruct.2015.11.043

[27] W. Zhuo, T. Tong, and Z. Liu, "Analytical pushover method and hysteretic modeling of precast segmental bridge piers with high-strength bars based on cyclic loading test," *Journal of Structural Engineering*, Vol. 145, No. 7, p. 04019050, Jul. 2019, https://doi.org/10.1061/(asce)st.1943-541x.0002318

[28] W.-D. Zhuo, Z. Liu, J.-D. Zhang, and W.-M. Zhang, "Comparison study on hysteretic energy dissipation and displacement components between cast-in-place and precast piers with high-strength

bars," *Structural Concrete*, Vol. 19, No. 3, pp. 747–757, Jun. 2018, https://doi.org/10.1002/suco.201700050

[29] W. Zhuo, Z. Liu, Z. He, and J. Zhang, "Seismic evaluation of precast piers with different rebar strength based on characterized resilience parameters," *Journal of Testing and Evaluation*, Vol. 47, No. 4, pp. 20170519–2978, Jul. 2019, https://doi.org/10.1520/jte20170519

[30] W. Zhuo, Z. Liu, W. Zhang, and J. Zhang, "Experimental Study on Ductility and Hysteretic Energy of CIP and Precast Bridge Piers with High Strength Rebar," in *IABSE Symposium, Vancouver 2017: Engineering the Future*, pp. 81–87, 2017, https://doi.org/10.2749/vancouver.2017.0081

[31] T. Tong, W. Zhuo, X. Jiang, H. Lei, and Z. Liu, "Research on seismic resilience of prestressed precast segmental bridge piers reinforced with high-strength bars through experimental testing and numerical modelling," *Engineering Structures*, Vol. 197, p. 109335, Oct. 2019, https://doi.org/10.1016/j.engstruct.2019.109335

[32] Y. Zhang, G. Wu, and D. Dias-Da-Costa, "Cyclic loading tests and analyses of posttensioned concrete bridge columns combining cast-in-place and precast segments," *Bulletin of Earthquake Engineering*, Vol. 17, No. 11, pp. 6141–6163, Nov. 2019, https://doi.org/10.1007/s10518-019-00714-0

[33] Y. Zhang, A. Tabandeh, Y. Ma, and P. Gardoni, "Seismic performance of precast segmental bridge columns repaired with CFRP wraps," *Composite Structures*, Vol. 243, p. 112218, Jul. 2020, https://doi.org/10.1016/j.compstruct.2020.112218

[34] T. Tong, S. Yuan, W. Zhuo, and Z. Liu, "Experimental and numerical investigations on cyclic behaviors of precast segmental bridge piers with the hybrid of high-strength bars and unbonded prestressing tendons," *Advances in Structural Engineering*, Vol. 24, No. 3, pp. 509–521, Feb. 2021, https://doi.org/10.1177/1369433220956814

[35] H. Jiang, C. Li, X. Bai, and G. Song, "Seismic performance analysis of precast segmental bridge columns with self-centering energy dissipation device," in *International Conference on Smart Transportation and City Engineering*, Vol. 12050, pp. 978–988, Nov. 2021, https://doi.org/10.1117/12.2613685

[36] Y. Ni, C. Hao, and Y. Xu, "Seismic performance analysis of self-centering segment piers with mortise-tenon shear connectors based on cyclic pseudo-static test," *Journal of Vibroengineering*, Vol. 23, No. 7, pp. 1621–1639, Nov. 2021, https://doi.org/10.21595/jve.2021.22029

[37] Y. Y. Song, "Research on seismic performance of segmental bridge piers with external energy-dissipation plates," (in Chinese), Southeast University, 2018.

[38] K. Kawashima, G. A. Macrae, J.-I. Hoshikuma, and K. Nagaya, "Residual displacement response spectrum," *Journal of Structural Engineering*, Vol. 124, No. 5, pp. 523–530, May 1998, https://doi.org/10.1061/(asce)0733-9445(1998)124:5(523)

[39] Z. X. Li, "Experimental and numerical analysis study on seismic performance of segmental assembled round end hollow piers," (in Chinese), Beijing Jiaotong University, 2021.

Hao Li graduated from School of Civil Engineering of Beijing Jiaotong University, who mainly engaged in the research on the seismic performance of precast assembled railway pier. Now he is a bridge engineer of Beijing Urban Construction Design and Development Group Co., Ltd.

Yuanqing Xu, senior engineer. In 2009, he graduated from Jilin University with a bachelor's degree in bridge engineering. In 2012, he graduated from Beijing Jiaotong University with a master's degree in bridge and tunnel engineering. Now, he is studying for a doctor's degree in the college of civil engineering of Hunan University and serves as the laboratory director of CCCC Highway Bridge National Engineering Research Centre Co., Ltd. His research direction is the structural system and seismic isolation technology of long-span bridges.

Hongjie Zhang, Professor level senior engineer, serves as the deputy director of the third Institute of Rail Transit Design and Research Institute of Beijing Urban Construction Design and Development Group Co., Ltd. He has been engaged in the design and seismic research of rail transit bridges for a long time and participated in the design of rail bridges in many cities in China as the principal. In addition, he has compiled many design specifications for urban rail transit bridges, such as code for design of urban rail transit bridge, etc.

Shiyun Qi is a graduate student at School of Civil Engineering of Beijing Jiaotong University, who mainly engaged in the research on seismic performance analysis and engineering economy study of railway pier under rare earthquake and near fault earthquake.